



A stereovision system for three-dimensional measurements of machines

Marek Grudziński, Łukasz Marchewka 

West Pomeranian University of Technology
Department of Mechanical Engineering and Mechatronics
17 Piastów Ave., 70-310 Szczecin, Poland
e-mail: mgrudzinski@zut.edu.pl, lukasz.marchewka95@gmail.com
 corresponding author

Key words: stereovision system, machine vision, camera tracking, camera calibration, calibration pattern, 3D reconstruction

Abstract

The modern manufacturing or transportation machines that are used in industrial processes require continuous supervision in certain circumstances and even manual control by a human. Despite the fact the machines are more and more reliable and accurate than they used to be there is still the need for manual and time-consuming programming and safety control, especially when the external conditions change. For the operation of large machines, where the risk of damage and even disaster exists, an additional supervisory system based on vision devices could be utilized. The vision systems are commonly used in a range of simple 2D detection as well as very precise 3D reconstruction. The stereovision systems could be applied for unusual operations, especially in terms of safety and collision avoidance, such as crane observations while transporting a heavy load, robot and CNC machine preparation and normal operation. Through the use of optical devices the observed objects could be quickly positioned. In this research a test bench for stereovision reconstruction for the example of a robotic arm has been presented. The calibration procedures have been explained and accuracy tests in a large measuring volume were performed. Finally the possibilities of the applications and the utilization of such a system have been assessed.

Introduction

The modern machines used in advanced transportation or manufacturing technologies allow for fast and accurate operations, supporting the operator. Many industrial devices are powered by efficient electric or hydraulic servo drives. However, despite the overall development of the robotics, some of them are still fully dependent on a human's decisions, e.g. cargo motions by individual movements of each arm of the special crane, mounted on trucks or excavators. Although the machines are equipped with additional supporting systems for the operator, which help to make the right decisions and speed up the processes, industrial practice has revealed that more than half of the time is wasted programming the machine, positioning and fastening the load or workpiece, carrying out quality control, etc.

In a Computer Numerical Control (CNC) machine the operator has to manually mount the workpiece in the proper position by the use of special measuring tools like a touch-probe. The arms of more advanced industrial robot, equipped with vision sensors, are capable of recognizing objects, and are able to move within a given trajectory and selected points and can be programmed faster (Pan et al., 2012). A problem appears when the conditions in the workspace changes and there are difficulties in the manual programming of the manipulator's movements, e.g. variable cargo distributions.

At the same time, noticeable development of vision techniques for image processing and precise measurement has been observed and so called "machine vision" systems have become more and more prevalent. The common term "machine vision" describes all the techniques that perform various tasks

based on the images captured by cameras. A particular group of such devices, called 3D scanners, can achieve the same accuracy of modern CNC machines and allow the quality of manufactured objects to be controlled to within less than one minute. Most of the industrial vision systems are used to increase the efficiency of production and to improve the quality control; reducing or eliminating the human factor. One of the modern solutions is the augmented reality technique (AR) which allows for more intuitive programming and understanding of the machine's operations (Olwal, Gustafsson & Lindfors, 2008). However accurate and high-resolution measurements cannot be performed with the use of freely moving cameras mounted on a head-display. The most advanced vision systems have been applied in serial production and for the efficient control of manufactured details, i.e. automotive parts. There are also other solutions for 3D scanning of machines in real-time, such as laser trackers or Lidar systems (Miądlicki, Pajor & Saków, 2017), but they cannot track and position multiple objects at the same time with high accuracy, or recognize image details such as shapes, edges or colors and they are relatively expensive.

One particular group of industrial and laboratory vision devices are those equipped with one or more integrated cameras, which simultaneously observe the workspace from different positions; this means that stereoscopic spatial observations are possible. The main issue with the system is to determine the geometric relation between the camera's coordinate system and the machine's coordinate system in one space. In special cases additional illuminators are designed to project a series of light patterns, enabling 3D scanning of the object's geometry. These systems allow for the creation of a complex high-resolution 3D model and compare the geometry in reference to the CAD model. Using the dedicated camera calibration procedures and software for image processing and marker detection, the 3D reconstruction of selected points in the workspace might be possible.

In this research work the general concept of a supervisory optical device which could be integrated with several types of machines has been presented. A number of advanced procedures for image acquisition and processing, as well as for the calibration of the cameras and 3D reconstruction with the help of coded markers have been developed. Finally a series of measurements in a large volume have been carried out using a prepared length pattern (scale-bar) and an industrial robot.

Camera calibration

The most commonly used pinhole model for camera calibration is based on the so called perspective projection technique. According to Figure 1, the camera model includes the so called *intrinsic parameters* i.e. focal length f , cross point (cc_m, cc_n) of the Charge-Coupled Device (CCD) and the main optical axes, the sensor skewness γ , as well as the so called *extrinsic parameters*, i.e. the orthogonal rotation matrix R and the translation vector t in relation to the specified world coordinate system T , associated with the calibration pattern.

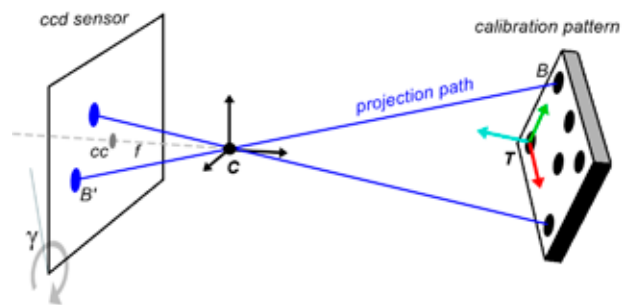


Figure 1. Simple projection of the calibration points

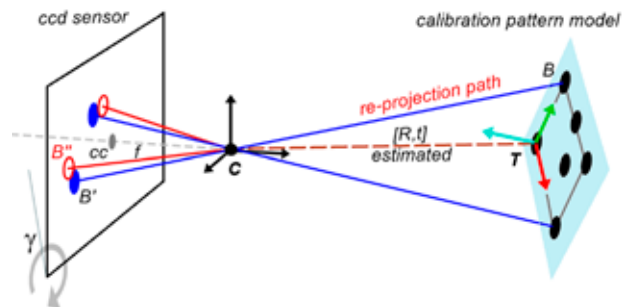


Figure 2. Re-projection of the modelled calibration pattern

The projection B' of the selected 3D point B to a flat image sensor can be described with the so called homography matrix H including both types of camera parameters, which can be written as the following equation:

$$\mathbf{B}' = \mathbf{H}\mathbf{B} \tag{1}$$

where:

$$\mathbf{H} = \mathbf{A}\mathbf{c} \cdot \mathbf{R} | \mathbf{t} = \begin{bmatrix} f_m & \gamma & cc_m & 0 \\ 0 & f_n & cc_n & 0 \\ 0 & 0 & 1 & 0 \\ 0 & 0 & 0 & 1 \end{bmatrix} \cdot \begin{bmatrix} R_{11} & R_{12} & R_{13} & t_x \\ R_{21} & R_{22} & R_{23} & t_y \\ R_{31} & R_{32} & R_{33} & t_z \\ 0 & 0 & 0 & 1 \end{bmatrix},$$

$$\mathbf{B}' = \begin{bmatrix} B'_m \\ B'_n \\ 1 \\ 1 \end{bmatrix}, \quad \mathbf{B} = \begin{bmatrix} B_x / B_z \\ B_y / B_z \\ B_z / B_z \\ 1 \end{bmatrix} \tag{2}$$

During camera calibration a reverse task is performed, resulting in a new homography based on the set of defined 3D points B in T space and their projections B' on the camera sensor. A group of B points can represent a calibration pattern, e.g. chessboard corners or a raster of circular dots. As shown in Figure 2, the full camera model is estimated iteratively by minimizing the so called *re-projection errors*, which mean the deviations of the projected on CCD points B' to their modeled equivalents on image B'' (Zhang, 1999). Therefore, the intrinsic parameters are strongly dependent on the precision of the calibration pattern, as well as the points' detection accuracy on the images.

In this research for intrinsic parameters calibration, a regular chessboard with a size of 600×450 mm has been designed and mounted on a rigid aluminum frame (Figure 3). The calibration parameters have been computed using the modified calibration toolbox for Matlab (Bouguet, 2010) (Figure 4). This procedure can be performed once outside the machines workspace, or in case of repeated measuring errors.

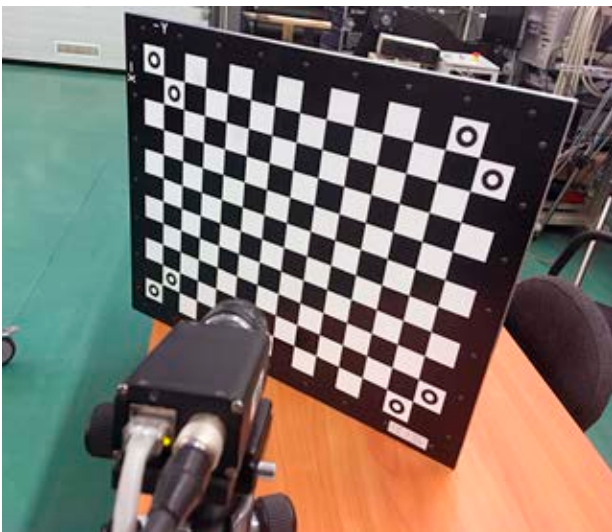


Figure 3. Calibration pattern for the camera's intrinsic parameters

```
>> Ac
Ac(:,:,1) =
  1.0e+03 *
    2.9169   -0.0000   0.7976
     0       2.9163   0.6320
     0         0       0.0010
Ac(:,:,2) =
  1.0e+03 *
    2.9075   -0.0000   0.8055
     0       2.8724   0.6598
     0         0       0.0010

>> Kc
Kc(:,:,1) =
 -0.0900
  0.3552
 -0.0001
 -0.0005
     0
Kc(:,:,2) =
 -0.0999
  0.4510
  0.0011
  0.0014
     0
```

Figure 4. Example of the obtained camera's parameters

Stereo pair calibration

The extrinsic parameters have to be determined directly in the workspace for both cameras simultaneously by the use of the same homographic transformation. If the calibration pattern geometry and its projections on both CCD sensors are known then new rotations and translations can be estimated. Due to the long relative distance between the cameras, another calibration pattern needed to be used, that allowed for undisturbed observation from two different positions (Luhmann et al., 2006). The calibration pattern was constructed in the shape of a regular cross, and carried a group of at least 9 coded markers on its arms. The precision of the pattern's assembly was not a crucial factor, since the relations between all the coded markers were calibrated by the use of a GOM Tritop photogrammetry system (Figure 5). Considering the possible disturbances that can be caused by ambiguous lighting, reflection of artificial light sources etc. all markers were printed on matte paper.

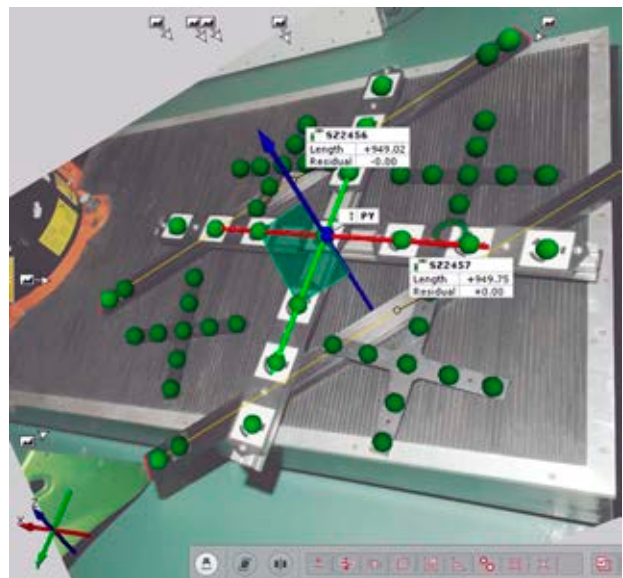


Figure 5. Photogrammetric measurement of the calibration cross in the GOM System

A stereo pair of cameras were mounted on one common aluminum beam and locked in stable positions. Since the relation of both cameras did not change, the measuring system could be freely displaced in the machine workspace. Only one calibration of the extrinsic parameters was needed for any measurements from any point of view. In order to evaluate the calibration results, a simple visualization including the cameras' positions and the observations' cones was developed in Matlab (Figure 6).

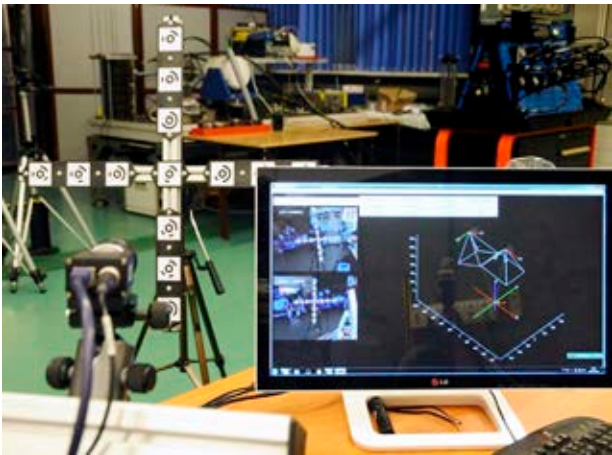


Figure 6. Visualization of the extrinsic parameters in a Matlab window

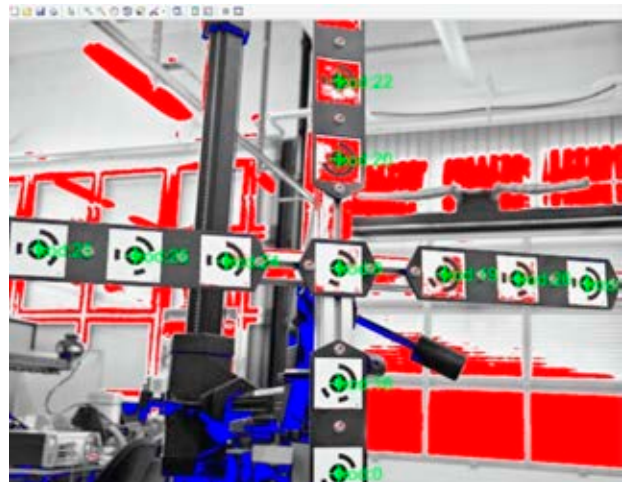


Figure 7. The detection of the coded markers in the presence of a detailed background and various lighting conditions

Marker detection

For the purpose of calibration and machine scanning, a group of points needed to be attached to the real objects and identified on the images. Flat, round markers were proposed which could be equally illuminated and always appear as high contrast regular ellipses on an image. In the first step the proposed algorithm searches for the objects with common centers of gravity, and then fits the exact ellipse model. Furthermore, the binary 7-bits Gray Code sequences were placed around the circular area, which allowed each marker to be distinguished among the others.

After the combination of a unique *start bit sequence* of 1-0-0, the following 7 segments (bits) allowed for the design of 54 different codes. Several tests were performed successfully to define the markers' best shape and proportions to detect their appearance in a detailed environment (Figure 7). Additional restrictions for image thresholding, the size of the detected segments and the proper exposure times were applied in the final algorithm.

An original solution for fast code detection was developed in Matlab (Figure 8). After the detection of the elliptical central marker, the algorithm performs a series of steps based on a binary representation of



Figure 8. An example of the segments that were prequalified as potential markers (blue circles and red crosses)

the image area around the marker (Figure 9). There are five steps as follows:

- boundary detection and cleaning for the center marker;
- morphological *shrink* operation resulting in a one-pixel thin pattern, elliptical model alignment and tilt angle detection;
- rotation of the segment from step a) and determination of the marker's proportion;
- cutting an image area with code segments based on the proportion from c) and the rotation based on b);
- scaling of the selected area to the shape of a square and code reading.

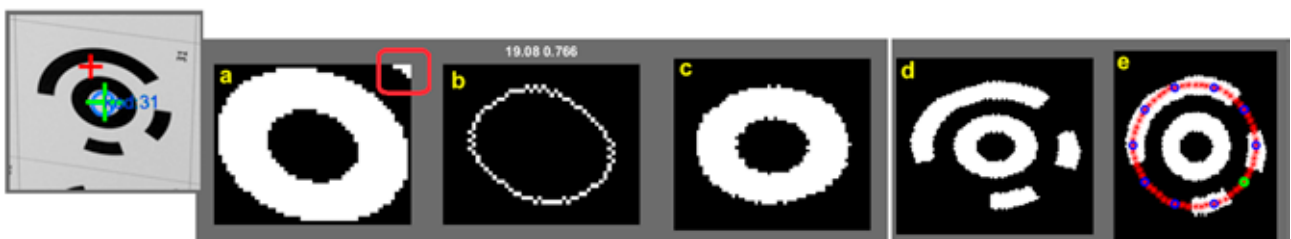


Figure 9. Procedures in the code detection for identified concentric segments

The last and more complicated step e) consists of another operation's subsequence; the main tasks of which are the location of the start bit sequence and the following bits. This could be performed after image sampling occurred around the central marker with a constant angle of 36°. The read binary code was then converted to decimal code and presented on the image.

Fundamental mathematics in 3D reconstruction

One of the main goals of the proposed vision system is the calculation of 3D coordinates for characteristic points attached to the observed machine and detected on two stereo images. At least two cameras are necessary for the reconstruction of the points' third dimension, which is normally lost during the image projection on the CCD sensor. For corresponding points, the so called inverse camera model and inverse projection are applied (3). In the research an original algorithm has been developed, where the calculations were based on both the intrinsic and extrinsic parameters and the known correspondence of each point.

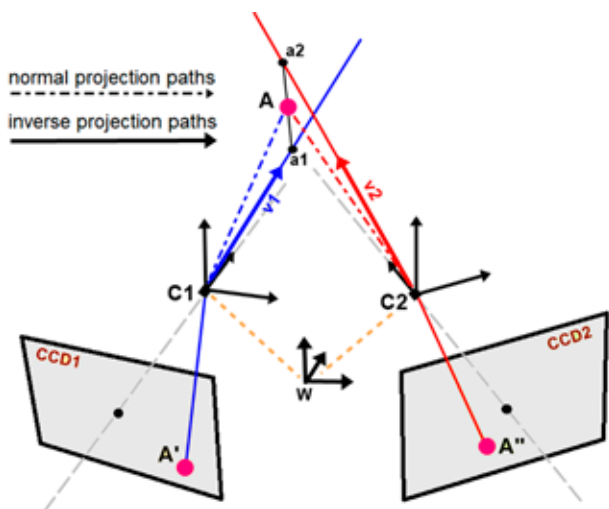


Figure 10. General idea of the 3D point reconstruction

$$\begin{bmatrix} v_x / v_z \\ v_y / v_z \\ 1 \end{bmatrix} = \mathbf{A}c^{-1} \cdot \mathbf{R}^{-1} \cdot \begin{bmatrix} A'_m \\ A'_m \\ 1 \end{bmatrix} + \begin{bmatrix} C_x \\ C_y \\ C_z \end{bmatrix} \quad (3)$$

As shown in Figure 10, the inverse camera model assumes that a selected point A can be projected from the CCD sensor to the 3D space in the form of vectors, $v1$ and $v2$, attached to the camera's coordinate systems $C1$ and $C2$, and translated and rotated

according to the actual extrinsic parameters in W . Two constructed lines, based on the inverse projections for both cameras, should intersect in the 3D space, indicating a searched 3D point A . In the practical solutions the lines pass by each other, missing by a very small value as a result of the estimated camera models and calibrations errors. The task is to find the shortest distance $a1$ to $a2$ for which the middle point is able to estimate the point A . For this purpose the following matrix equation was applied:

$$g1 \cdot \begin{bmatrix} v1_x \\ v1_y \\ v1_z \end{bmatrix} + \begin{bmatrix} C1_x \\ C1_y \\ C1_z \end{bmatrix} + g \cdot \begin{bmatrix} vc_x \\ vc_y \\ vc_z \end{bmatrix} + \left(g2 \cdot \begin{bmatrix} v2_x \\ v2_y \\ v2_z \end{bmatrix} + \begin{bmatrix} C2_x \\ C2_y \\ C2_z \end{bmatrix} \right) = \begin{bmatrix} 0 \\ 0 \\ 0 \end{bmatrix} \quad (4)$$

This solved the problem of adding three perpendicular vectors in 3D space and scaling by unknown g -factors. The vc vector's coordinates was obtained by applying a cross-product for $v1$ and $v2$. The scale factors $g1$ and $g2$ allowed for the 3D coordinates of $a1$ and $a2$ points to be determined, for which the average value determined the reconstructed point A , given by:

$$\begin{bmatrix} A_x \\ A_y \\ A_z \end{bmatrix} = 0.5 \cdot \left(g1 \cdot \begin{bmatrix} v1_x \\ v1_y \\ v1_z \end{bmatrix} + \begin{bmatrix} C1_x \\ C1_y \\ C1_z \end{bmatrix} + g2 \cdot \begin{bmatrix} v2_x \\ v2_y \\ v2_z \end{bmatrix} + \begin{bmatrix} C2_x \\ C2_y \\ C2_z \end{bmatrix} \right) \quad (5)$$

Testing the accuracy of the 3D reconstruction

For the new established extrinsic parameters for a stereo pair of cameras, a 3D reconstruction test was carried out. When considering a large measuring volume, a good solution is to not only measure the position of a single point, but measure the well-known distance of two points. Such an approach is commonly used to verify the accuracy of 3D scanners and photogrammetric systems, according to VDI/VDE 2634 standards (Ostrowska, Szewczyk & Sładek, 2012). A simple length pattern with two coded markers was created and attached to an aluminum beam. The reference distance of 1124.56 mm was measured by the use of the GOM Tritop system (Figure 11).

During the tests the length pattern was placed in front of the cameras (Figure 12) in five positions and

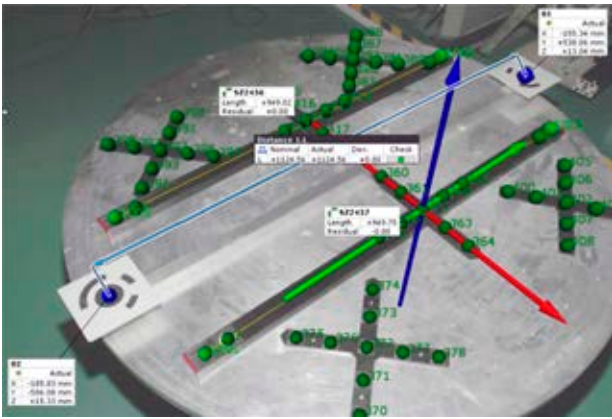


Figure 11. The Scale-bar during calibration



Figure 12. Test of the reference distance measurement

at three different distances in relation to the world coordinate system, according to the scheme shown in Figure 13. The pair of markers was identified, reconstructed in 3D space and the Cartesian distance was calculated for each position of the pattern. The results have been presented in Table 1. In the planes -0.3 and 0 m, the smallest average deviations of $1-1.5$ mm were observed. The deviations were expected to be slightly smaller than 1 mm, however the results strongly depended on the intrinsic parameters calibrations, especially the image distortion coefficients.

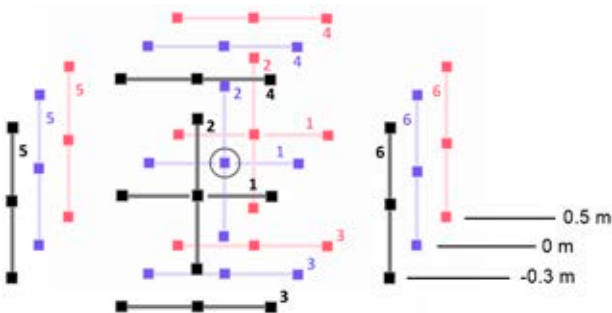


Figure 13. Arrangement of the length pattern positions. Center point of the measuring volume marked with a circle

Table 1. Results of the measurements for the length pattern

Position	1	2	3	4	5	6
plane -0.3 m						
Distance [mm]	1125.4	1125.4	1123.5	1123.7	1122.2	1122.4
Deviation [mm]	0.8	0.8	1.1	0.9	2.4	2.2
plane 0 m						
Distance [mm]	1123.2	1123.4	1123.5	1122.8	1124.1	1124.3
Deviation [mm]	1.4	1.2	1.1	1.8	0.5	0.3
plane 0.5 m						
Distance [mm]	1121.9	1124.3	1120.0	1119.4	1122.1	1122.3
Deviation [mm]	2.7	0.3	4.6	5.2	2.5	2.3

Measurements of the robot's end effector positions

As a part of the initial study of the large space optical measurement, an experiment was carried out with the use of the cameras and an industrial robot with a serial kinematic structure. The experiment in general consisted of taking position measurements of the reference marker mounted on the robot's end effector and then comparing them to the reference positions. The preparations for the tests were preceded by calibration of the extrinsic parameters for the two cameras using the reference cross. In the next step a measurement of the relation of the cameras to the robot's coordinate system was carried out, which consisted of several straight movements of the end effector along two of the robot's main axes and simultaneously capturing these movements with the stereo cameras. The recorded markers' paths allowed for the definition of a local coordinate system R , in which other measurements of several points was performed (Figure 15).



Figure 14. Example of a correct and incorrect potential marker with concentric fields

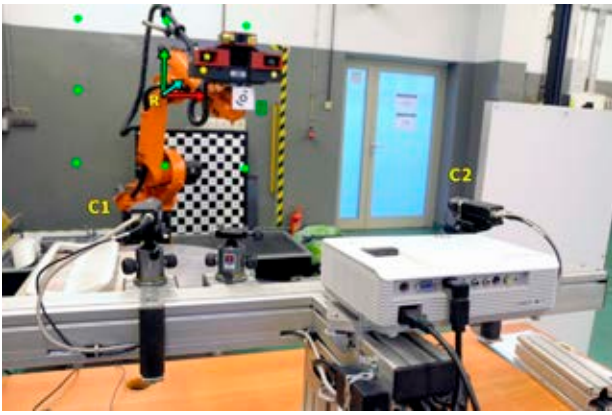


Figure 15. Reference points (green dots) programmed in the robot's space *R*

The observed point was a circular flat coded marker, No. 8 (Figure 14). The measuring volume was determined as a cube with a side length of 500 mm. The position of the marker was measured in the 27 programmed positions of the end effector, and assigned to three planes within the cube (near, central and far). The center point of the cube was positioned at a distance of about 3 m from the cameras and the distance between the cameras was set to 1.2 m. Due to the specification and the current technical condition of the robot, the positioning accuracy of the robot was set to 0.2 mm, assuming that it was not under any load (Figure 16).

The average position error was ca. 0.5 mm at the center of the measuring volume and it increased up to a maximum value of 3 mm at the boundaries.

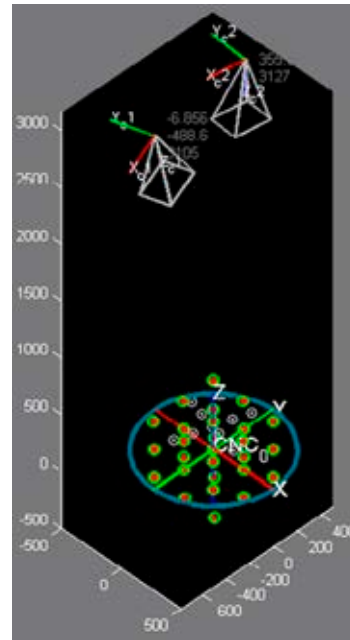


Figure 16. Cameras, reference and measured points in the same local coordinate system *R*

The experiment confirmed the satisfactory accuracy of the vision positioning of the robot using the original implemented algorithms, considering that the measuring distance was much greater than in the commonly used close range systems. It also showed small systematic deviations, resulting in a small skewness of the measuring space (Figure 18), probably caused by a too small calibration pattern and uncorrected image distortions. The observed systematic error was used for experimental correction

REF X [mm]	dev X [mm]	REF Y [mm]	dev Y [mm]	REF Z [mm]	dev Z [mm]	dev. XYZ [mm]	dev. XYZ with correction [mm]
-250.93	-0.93	-250.44	-0.44	247.95	-2.05	2.29	1.53
-1.41	-1.41	-250.84	-0.84	248.91	-1.09	1.97	1.75
248.50	-1.50	-250.31	-0.31	249.50	-0.50	1.61	1.56
-251.01	-1.01	-1.59	-1.59	248.57	-1.43	2.36	2.10
-1.40	-1.40	-1.75	-1.75	248.60	-1.40	2.64	2.24
248.65	-1.35	-1.27	-1.27	249.34	-0.66	1.97	1.81
-251.15	-1.15	249.10	-0.90	248.93	-1.07	1.81	1.74
-1.47	-1.47	248.69	-1.31	248.65	-1.35	2.38	1.89
248.72	-1.28	249.49	-0.51	248.53	-1.47	2.01	0.99
-250.10	-0.10	-249.97	0.03	-0.50	-0.50	0.51	0.69
-0.42	-0.42	-249.82	0.18	-0.08	-0.08	0.47	0.43
248.98	-1.02	-249.71	0.29	0.94	0.94	1.42	1.16
-250.03	-0.03	-0.23	-0.23	0.07	0.07	0.24	0.46
-0.43	-0.43	-0.05	-0.05	-0.03	-0.03	0.44	0.44
249.26	-0.74	0.03	0.03	0.20	0.20	0.77	0.44
-250.25	-0.25	249.94	-0.06	0.10	0.10	0.27	0.62
-0.46	-0.46	249.91	-0.09	-0.19	-0.19	0.50	0.50
249.35	-0.65	250.37	0.37	0.00	0.00	0.74	0.58
-249.08	0.92	-248.25	1.75	-248.46	1.54	2.51	1.72
0.52	0.52	-248.23	1.77	-248.81	1.19	2.20	1.74
250.23	0.23	-247.96	2.04	-248.03	1.97	2.84	2.06
-248.97	1.03	1.41	1.41	-247.87	2.13	2.75	1.70
0.51	0.51	1.64	1.64	-248.48	1.52	2.30	1.72
250.40	0.40	1.83	1.83	-248.90	1.10	2.17	2.01
-249.09	0.91	251.31	1.31	-248.34	1.66	2.30	1.56
0.43	0.43	251.58	1.58	-249.00	1.00	1.92	1.82
250.41	0.41	251.91	1.91	-248.91	1.09	2.24	2.22

Figure 17. Coordinates of the robot's end effector measured by the stereo camera system

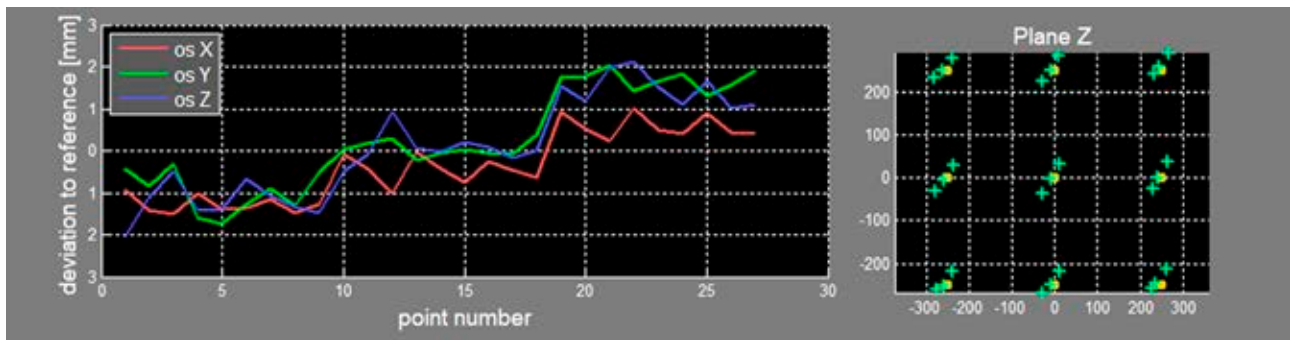


Figure 18. Deviations of the measured points in three dimensions; separately (left) and a composition of the deviation error in the X and Y axes (enlarged 10-times)

of the measurements, which improved the results by about 30% (Figure 17).

Conclusions

The authors of this paper have proposed a new solution to integrate the vision system and a machine with known kinematics, which in future applications could improve on time-consuming manual programming. The initial position of the machine and the calibration of the common workspace with the vision system are sufficient, on the condition that the calibration pattern or group of reference points have been mounted precisely in a well-established position relative to the machine's coordinate system. This allows to scan and measure points in the common coordinate system both for scanner and the machine.

One of the conclusions of the tests was a positive evaluation of the stereovision system for application in a large volume of space. However, measurements with higher accuracy require a bigger and more precise calibration pattern and the further development of algorithms for image distortion corrections. Wide-angle lenses could observe a higher space, but the main problems in such a solution are significant image distortions and low pixel resolutions in standard cameras. Although the passive flat markers were useful for the research, they might be insufficient for multi-direction observations in a difficult industrial environment. Much more useful would be groups of active markers based on a pulse-coded Near-Infrared (NIR) light source.

In other possible applications the system could be used for inverse kinematics calculations and much easier and intuitive control of the machine e.g. loading cranes or excavators (Pajor, Grudziński & Marchewka, 2018). For very large volumes the system could track and control the positions of self-acting transport devices, such as gantry cranes or mobile robots. The stereovision system could

also be utilized in CNC machines by manual programming of the basic movements as well as for the determination of base coordinate systems for manufacturing or the safety space for the tool. Additional hand tools for vision measuring of the workpiece would be suggested for inaccessible surfaces. For more accurate positioning for precise machines such as CNC machines, further tests in terms of error estimations would need to be performed (Majda & Pajor, 2016).

References

1. BOUGUET, J.Y. (2010) *Camera calibration toolbox for Matlab*.
2. LUHMANN, T., ROBSON, S., KYLE, S. & HARLEY, I. (2006) *Close Range Photogrammetry: Principles, Methods and Applications*. Whittles Publishing.
3. MAJDA, P. & PAJOR, M. (2016) *Szacowanie niepewności pomiaru przestrzennego błędu pozycjonowania maszyn technologicznych*. *Mechanik* 11, pp. 1546–1550.
4. MIĄDLICKI, K., PAJOR, M. & SAKÓW, M. (2018) Loader Crane Working Area Monitoring System Based on LIDAR Scanner. In: Hamrol A., Ciszak O., Legutko S., Jurczyk M. (Eds) *Advances in Manufacturing. Lecture Notes in Mechanical Engineering*. Springer, Cham, pp. 465–474.
5. OLWAL, A., GUSTAFSSON, J. & LINDFORS, C. (2008) *Spatial augmented reality on industrial CNC-machines*. Proceedings of SPIE 2008 Electronic Imaging, Vol. 6804 (The Engineering Reality of Virtual Reality 2008), San Jose, CA, January 27–31, 2008.
6. OSTROWSKA, K., SZEWCZYK, D. & SŁADEK, J. (2012) Wzorcowanie systemów optycznych zgodnie z normami ISO i zaleceniami VDI/VDE. *Mechanika* 109, z. 9-M, pp. 167–179.
7. PAJOR, M., GRUDZIŃSKI, M. & MARCHEWKA, Ł. (2018) *Stereovision system for motion tracking and position error compensation of loading crane*. AIP Conference Proceedings 2029, 020050.
8. PAN, Z., POLDEN, J., LARKIN, N., VAN DUIN, S. & NORRISH, J. (2012) Recent Progress on Programming Methods for Industrial Robots. *Robotic and Computer Integrated Manufacturing* 28, (2), pp. 87–94.
9. ZHANG, Z. (1999) *Flexible camera calibration by viewing a plane from unknown orientations*. Proceedings of the 7th International conference on Computer Vision, 20–27 Sept. 1999, Kerkyra, Greece.